Published in final edited form as:
Int J Biochem Cell Biol. 2012 November ; 44(11): 1852–1861. doi:10.1016/j.biocel.2012.06.025.

Delineating Metabolic Signatures of Head and Neck Squamous Cell Carcinoma: *Phospholipase A_2*, a Potential Therapeutic Target

Pratima Tripathi[1,#], **Pachiyappan Kamarajan**[2,#], **Bagganahalli S. Somashekar**[1], **Neil MacKinnon**[1], **Arul M. Chinnaiyan**[3,4,5,6], **Yvonne L. Kapila**[2], **Thekkelnaycke M. Rajendiran**[3], and **Ayyalusamy Ramamoorthy**[1,*]

[1]Department of Chemistry and Biophysics, School of Dentistry, University of Michigan, Ann Arbor, Michigan, United States

[2]Department of Periodontics and Oral Medicine, School of Dentistry, University of Michigan, Ann Arbor, Michigan, United States

[3]Michigan Center for Translational Pathology, Department of Pathology, University of Michigan Medical School, Ann Arbor, Michigan, United States

[4]Department of Urology, University of Michigan Medical School, Ann Arbor, Michigan, United States

[5]Comprehensive Cancer Center, University of Michigan Medical School, Ann Arbor, Michigan, United States

[6]Howard Hughes Medical Institute, University of Michigan Medical School, Ann Arbor, Michigan, United States

Abstract

A better understanding of molecular pathways involved in malignant transformation of head and neck squamous cell carcinoma (HNSCC) is essential for the development of novel and efficient anti-cancer drugs. To delineate the global metabolism of HNSCC, we report ^{1}H NMR-based metabolic profiling of HNSCC cells from five different patients that were derived from various sites of the upper aerodigestive tract, including the floor of mouth, tongue and larynx. Primary cultures of normal human oral keratinocytes (NHOK) from three different donors were used for comparison. ^{1}H NMR spectra of polar and non-polar extracts of cells were used to identify more than thirty-five metabolites. Principal component analysis performed on the NMR data revealed a clear classification of NHOK and HNSCC cells. HNSCC cells exhibited significantly altered levels of various metabolites that clearly revealed dysregulation in multiple metabolic events, including Warburg effect, oxidative phosphorylation, energy metabolism, TCA cycle anaplerotic

[*]Corresponding Author: Prof. Ayyalusamy Ramamoorthy, Biophysics and Department of Chemistry, University of Michigan, 930 North University Avenue, Ann Arbor, Michigan 48109-1055, USA, Phone: (734) 647-6572, Fax: (734) 764-3323, ramamoor@umich.edu.
[#]Authors contributed equally

Disclosure
No conflict of interest to declare.

Supporting content: Supplementary data associated with this article can be found, in the online version.

flux, glutaminolysis, hexosamine pathway, osmo-regulatory and anti-oxidant mechanism. In addition, significant alterations in the ratios of phosphatidylcholine/lysophosphatidylcholine and phosphocholine/glycerophosphocholine, and elevated arachidonic acid observed in HNSCC cells reveal an altered membrane choline phospholipid metabolism (MCPM). Furthermore, significantly increased activity of *phospholipase* A_2 (PLA_2), particularly *cytosolic* PLA_2 ($cPLA_2$) observed in all the HNSCC cells confirm an altered MCPM. In summary, the metabolomic findings presented here can be useful to further elucidate the biological aspects that lead to HNSCC, and also provide a rational basis for monitoring molecular mechanisms in response to chemotherapy. Moreover, $cPLA_2$ may serve as a potential therapeutic target for anti-cancer therapy of HNSCC.

Keywords

Head and Neck Squamous Cell Carcinoma; NMR spectroscopy; Metabolites; Lipids; Metabolomics; *phospholipase* A_2

1. Introduction

Head and neck squamous cell carcinoma (HNSCC) is an epithelial malignancy that arises in various sites of the upper aerodigestive tract encompassing lip, oral cavity, tongue, larynx, nasal cavity, paranasal sinuses and pharynx. HNSCC, the fifth most common type of cancer, represents about 6% of all cases, and it accounts for an estimated > 300,000 new cases worldwide every year (Rezende et al., 2010). The most important risk factors for HNSCC are tobacco use (smoked or chewed), alcohol consumption and human papillomavirus infection (Marur et al., 2010). The definitive diagnosis of HNSCC involves the use of multimodal approaches, including physical examination, endoscopy, radiography, computed tomography, magnetic resonance imaging, serum and urine analyses, and histopathological examination of tissue biopsies. The management of HNSCC is often complicated, involving multiple modes of therapy, including surgery, chemotherapy, and external beam radiation (Argiris et al., 2008). Moreover, disease prognosis significantly depends on the site and stage of the primary tumor, but survival rate remains poor for patients having solid aggressive tumors, and regional and distant metastases (Pignon et al., 2009).

A better understanding of the molecular pathways that lead to the development of head and neck neoplasia is essential for the development of novel and efficient anti-cancer therapies. In addition, the identification of potential molecular biomarkers of HNSCC could be clinically useful for predicting prognosis and therapeutic efficacy, and also in the development of targeted therapies. To better understand tumor metabolism of HNSCC, most studies have been carried out on HNSCC cells that have been cultured *in vitro* (Schmitz and Machiels, 2010, Sandulache et al., 2011, Jiffar et al., 2011), and tumor tissues obtained from *in vivo* conditions (Karahatay et al., 2007, Ziebart et al., 2011). Biomarkers associated with HNSCC that have been identified from tissues or serum/plasma, revealed considerable alterations in protein expression. These protein alterations represent different biochemical functions associated with the acquisition of a tumor phenotype (Rezende et al., 2010). We have recently reported that sirtuin-3 is overexpressed in oral squamous cell carcinoma, and it has been suggested as a novel potential therapeutic target for oral cancer (Alhazzazi et al., 2011). Complementary to these functional protein and genomics studies (Leemans et al., 2011), it is also important to understand the metabolic alterations, which occur during oncogenic transformation of HNSCC. However, the knowledge of metabolic pathways involved in malignant transformation of HNSCC is limited, and therefore warrants exploration. Thus, to explore and define tumor metabolism and to nominate potential biomarkers of HNSCC, we recently used Nuclear Magnetic Resonance Spectroscopy (NMR) to explore the metabolic signatures of HNSCC tissues originating from various sites

of the upper aerodigestive tract (Somashekar et al., 2011). In the present study, to further explore and confirm pathways altered during oncogenic transformation and to potentially identify novel therapeutic targets we carried out comprehensive NMR based metabolomics of various HNSCC cells and primary cultures of normal human oral keratinocytes (NHOK). We chose HNSCC cells derived from various sites of the upper aerodigestive tract, including the floor of mouth (UM-SCC-14A and UM-SCC-1), tongue (OSCC-3 and HSC-3), and larynx (UM-SCC-17B), and three NHOK from three different donors for comparison. In addition to the metabolic profiling of aqueous metabolites, we also carried out NMR analysis on lipid extracts of these cells to understand the global metabolism of HNSCC biology. The altered metabolites identified in the present study for HNSCC can be related to dysregulation of multiple pathways, including altered glucose metabolism, TCA anaplerotic flux, adaptive response to osmotic and oxidative stress, and energy metabolism. In addition, to explore the relationship between altered choline-containing metabolites and phospholipases, we assayed the total *phospholipase A_2 (PLA_2)* activity and specifically *cytosolic PLA_2 ($cPLA_2$)* activity. It is noteworthy that since both choline containing metabolites and PLA_2 are altered in HNSCC cells, a thorough understanding of the regulation of the phospholipase enzymes could bring significant insight to the altered MCPM pathway in HNSCC. We also postulate that PLA_2 could be a potential therapeutic target for anti-cancer therapy of HNSCC (Glunde and Serkova, 2006).

2. Materials and methods

2.1 Cell lines and cell culture

Five HNSCC cell lines originated from different sites of head and neck region and three different NHOK (K1, K2 and K3) were used in the present study. One of the NHOK (K1) was obtained from separated epithelial tissue of a de-identified donor specimen (discarded normal gingival tissue following periodontal surgery and Institutional Review Board exempt) and two NHOK (K2 and K3) were purchased from ScienCell (Carlsbad, CA). Highly invasive human oral squamous cell carcinoma (SCC) cell line HSC-3 was kindly provided by Dr. Randy Kramer (University of California, San Francisco). The human oral SCC cell lines, UM-SCC-1, UM-SCC-17B and UM-SCC-14A were gifts from Dr. Tom Carey (University of Michigan, Ann Arbor). The poorly differentiated aggressive tongue SCC cell line OSCC-3 was gift from Dr. Mark Lingen (University of Chicago, Chicago). HNSCC cells were incubated with Dulbecco's modified Eagle's medium (Gibco) supplemented with 10% fetal bovine serum, 1% penicillin, and 1% streptomycin in a 5% CO_2 atmosphere at 37°C. However, primary human oral keratinoctyes were incubated with oral keratinocyte medium (ScienCell, Carlsbad, CA) in a 5% CO_2 atmosphere at 37°C. Each cell line was grown independently in triplicates.

2.2 Aqueous and lipid metabolite extraction

2×10^6 cells were harvested from the culture flasks of each independently grown cell lines, cell pellets were washed thrice thoroughly with phosphate buffer and cell pellets were stored at −80 °C until used. The aqueous and lipids metabolites were extracted separately as described previously (MacKinnon et al., 2012). The aqueous cell extracts were reconstituted in 500 μL of deuterated 100mM phosphate buffer, while lipid extracts were reconstituted with 2:1 deuterated chloroform/methanol, transferred into 5 mm NMR tubes and used for NMR measurements.

2.3 NMR Experiments

All NMR measurements were carried out on a Bruker Avance 900 MHz NMR spectrometer (Bruker BioSpin, Karlsruhe, Germany) equipped with a 5mm HCN TCI cryo-probe at 298 K temperature. ^{1}H NMR spectra were acquired using a single 45° pulse experiment with water

presaturation during the relaxation delay. To assign peaks in the ^{1}H NMR spectra of the aqueous metabolites, two-dimensional (2D) ^{1}H-^{1}H total correlation spectroscopy (TOCSY) was performed on the aqueous extract of one of the HNSCC cell lines. The parameters used for 1D and 2D NMR experiments are given in supplementary information (Materials and methods).

2.4 Multivariate Statistical Analysis

Before subjecting the NMR spectra to PCA, the chemical shift region of 0.85–9.50 ppm was converted to ASCII-files and the spectral regions of residual water (4.62–5.45 ppm), regions where HEPES (2.94–2.97, 3.08–3.12, 3.13–3.17 and 3.85–3.88 ppm) and residual methanol (3.33–3.35 ppm) appear were removed. Similarly, in the case of NMR spectra of lipids, the spectral regions of residual water (4.34–4.60 ppm), methanol solvent signal (3.20–3.90 ppm) and the regions above 6.50 and below 0.50 ppm were removed. Spectral regions were normalized by the sum of all intensities over the entire sub-spectrum, and PCA was performed separately for NMR spectra of aqueous and lipid extracts with mean-centered scaling and full cross-validation (The Unscrambler V10.1, CAMO, Oslo, Norway). The results were presented as three-dimensional (3D) principal component scores plots (each point represents an individual sample), and loading plots in which metabolite peaks were shown as positive and negative signals to indicate differential changes of metabolites.

2.5 Relative Quantification and Statistical Analysis

For relative quantification, the intensities of metabolites were calculated separately for NHOK and HNSCC cells using total area normalized spectra and presented as mean ± standard deviation. The representative ^{1}H signal from each metabolite which is taken for relative quantification is underlined in Table S1 (Supplementary Information). Univariate statistical analysis was performed using SPSS statistical package version 11.5 (SPSS Inc., Chicago, IL, USA). Statistical comparisons were made using two-tailed Student's t-test followed by a correction for multiple hypothesis testing (Benjamini-Hochberg correction (Benjamini and Hochberg, 1995, Blaise et al., 2009)) at 5% level. Unsupervised hierarchical clustering (Pearson correlation) and heat map was drawn using R statistical package "gplot".

2.6 Total *PLA_2 and $cPLA_2$ activity assay*

Total PLA_2 activity was determined in whole cell lysates using the EnzChek® PLA_2 Assay Kit according to the manufacturer's instructions (E10217, Invitrogen, Eugene, OR, USA). To determine the activity of $cPLA_2$, secretory PLA_2 ($sPLA_2$) was removed from the whole cell lysate by using a membrane filter with a 30,000 Da molecular weight cut-off (Amicon centrifuge concentrator). To suppress the activity of intracellular Ca^{2+}-independent PLA_2 ($iPLA_2$), we used an $iPLA_2$ specific inhibitor, Bromoenol Lactone (5 μM), (765038, Cayman chemical company, Ann Arbor, MI, USA). Then, specifically, the $cPLA_2$ activity was measured with a $cPLA_2$ assay kit according to the manufacturer's instructions (765021, Cayman chemical company, Ann Arbor, MI, USA).

3. Results and discussion

Cancer cell lines are the most relevant and basic model systems of human cancer for exploring specific characteristics of metabolic mechanisms for various types of cancer. Data generated by metabolic profiling of individual cells is complementary to data obtained from analysis of the whole system, which can be directly correlated with genomics or proteomics data. Furthermore, the metabolomics data can be used for the development of models of biological pathways and networks. The aim of the present study was to delineate the global metabolism involved in malignant transformation of HNSCC by using ^{1}H NMR metabolic profiling of human cells derived from normal and HNSCC patients. In this regard, *in vitro*

grown HNSCC cells derived from three different anatomical sites (floor of mouth, larynx and tongue) from five donors were compared with NHOK (primary cultures) from three different donors. Both normal and HNSCC cells were cultured in triplicate, then aqueous (polar) metabolites were extracted from 2×10^6 cells, and ^{1}H NMR spectra were acquired for these samples as described in the methods section. In all nine of the ^{1}H NMR spectra of NHOK, signals from 4-(2-hydroxyethyl)-1-piperazineethanesulfonic acid (HEPES) were observed in spite of thorough washing of the cells thrice with phosphate buffered saline (PBS) solution. Visual inspection of these NMR spectra revealed that the relative intensities of HEPES signals to the rest of the metabolites were identical, indicating the definite adherence of HEPES to the cells; nevertheless the mechanism by which HEPES adheres to the cells is currently unknown. Therefore, HEPES was considered as an exogenous compound and the respective ^{1}H signals (2.94, 3.10, 3.15 and 3.86 ppm) were not considered for further analysis. On the whole, the metabolic profiles of HNSCC cells display unique metabolic signatures different from that of NHOK.

3.1 ^{1}H NMR profiles of polar metabolites reveal distinct metabolic signatures for HNSCC cells

^{1}H NMR spectra obtained from polar metabolites of NHOK and five different HNSCC cancer cells are shown in Figure 1. The ^{1}H NMR spectra from triplicate measurements of three individual NHOK cells showed identical spectral profiles. Therefore, the mean spectrum of all nine normalized NMR spectra was determined and is illustrated in Figure 1. Similarly, ^{1}H NMR spectra of the triplicates of each HNSCC cell type were also identical and thus the average spectrum of normalized values for each HNSCC cell is included in Figure 1. These observations highlight the excellent reproducibility and accuracy of aqueous metabolite extraction methodology of the independently grown cells. ^{1}H peak assignment of metabolites was achieved using a combination of previously reported chemical shifts (Somashekar et al., 2011), the Human Metabolome Database (HMDB) (Wishart et al., 2007) and the Biological Magnetic Resonance Data Bank (BMRB) (Cui et al., 2008), plus the assignment of peaks was further confirmed by 2D TOCSY (Figure 2). The metabolites unambiguously assigned were: isoleucine (Ile), leucine (Leu), valine (Val), lactate (Lac), alanine (Ala), lysine (Lys), acetate (Ac), N-Acetyl aspartate (NAA), glutamate (Glu), glutamine (Gln), pyruvate (Pyr), glutathione (GSH), aspartate (Asp), creatine (Cre), phosphocreatine (PCre), choline (Cho), phosphocholine (PCho), glycerophosphocholine (GPC), taurine (Tau), *myo*-inositol (*myo*-Ins), glycine (Gly), adenine mono/di/tri phosphate (AXP), uridine di-phosphate sugars (UDP-sugars), nicotinamide adenine dinucleotide (NAD^+), fumarate (Fum), tyrosine (Tyr), histidine (His), phenylalanine (Phe) and tryptophan (Trp). A complete list of chemical shift assignments of various metabolites is given in Table S1 (Supplementary Information). In total, more than 35 metabolites were identified, thus providing adequate information for assessing variations in metabolic pathways within normal and HNSCC cells.

To determine which cells shared global metabolic profile features, we performed principal component analysis (PCA), unsupervised hierarchical cluster analysis (Pearson correlation), and univariate analysis (Student's t-test). The ^{1}H NMR spectra of each cell grown independently in triplicates (24 NMR spectra) were subjected to unsupervised PCA. In the three-dimensional (3D) PCA scores plot (Figure 3A), triplicate samples of each cell type were grouped together, which demonstrates the reproducibility of the metabolic profile of each independently grown cell type. Also, the 3D PCA score plot (Fig. 3A) revealed a clear segregation of NHOK and HNSCC cells, wherein the principal components (PC) 1, 2 and 3 together explained 70% of data variation. While the three different NHOK grouped together, the five different HNSCC cells showed dispersed groupings which can be attributed to dynamic variations of metabolites between the cancer cell groups (Fig 3A). The loadings

plot for the first principal component (Fig 3B) revealed elevated levels of branched chain amino acids (leucine, isoleucine, valine), lactate, N-acetyl-aspartate, glutamate, creatine, phosphocreatine, choline, phosphocholine, taurine, *myo*-inositol, UDP-sugars, AXP, fumarate, tyrosine, phenylalanine, and decreased levels of alanine, acetate, glutamine, glutathione, aspartate, glycerophospholine and glycine.

Further, hierarchical clustering performed on the z-score of twenty-one quantified metabolites revealed that all the five HNSCC cancer cells cluster together and are well separated from the cluster of three NHOK (Fig. 4A). The heat map showing the variation of twenty-one metabolites (represented by z-score) of NHOK and HNSCC cells arranged by unsupervised hierarchical clustering are included in Fig 4A. The signal intensities of these twenty-one metabolites were compared between NHOK and HNSCC cells using Student's t-test followed by Benjamini-Hochberg correction, and P values are presented in Fig 4B. The signal intensities for all 21 metabolites were significantly different in HNSCC cells as compared to NHOK, with most metabolites showing $P < 0.001$ while other metabolites showed $P < 0.01$ and 0.05 (Fig. 4B).

3.2 ^{1}H NMR profile of non-polar metabolites reveals distinct metabolic signatures for HNSCC cells

The extracted lipid layer of all the cells were dried under vacuum and re-constituted in 600 μL 2:1 $CDCl_3$:CD_3OD (v/v) and ^{1}H NMR spectra were acquired. By visual inspection, each area-normalized ^{1}H NMR spectrum of the individual HNSCC triplicate data sets showed an identical spectral pattern, therefore the average of each HNSCC triplicate was determined and is depicted in Figure 5A. As in the case of the NHOK polar metabolite profiles, similarities were observed amongst all nine area-normalized spectra (three individual cell lines, each in triplicate) and thus the average of all nine spectra is depicted in Fig 5A. The spectral assignments were carried out using the combination of previously published chemical shift database of lipids (Adosraku et al., 1994) and ^{1}H NMR spectra of authentic lipid standards. The unambiguously assigned lipid metabolites in all the cell lines were cholesterol (Chol), polyunsaturated fatty acids [(PUFA), principally arachidonic acid], phosphatidycholine (PC), lysophosphatidylcholine (LysoPC) and sphingomyelin (SM).

Unsupervised PCA performed on the ^{1}H NMR spectra of the lipid extract of all the cells (Fig. 5B) revealed a clear group separation among NHOK and HNSCC cells, wherein PC 1, 2 and 3 together explained 70% of data variation. Even though all three NHOK showed a clear grouping, variations within HNSCC groups were observed due to relative variations in the altered lipids. To further probe the variations in the lipids quantitatively, the intensity of a representative peak for each lipid was calculated from the area-normalized spectra and compared between NHOK and each of the HNSCC groups (Student's t-test followed by Benjamini-Hochberg correction, Fig. 5C). The level of arachidonic acid was significantly elevated ($P < 0.001$), however, the PC:LysoPC ratio was significantly decreased ($P < 0.001$) in all cancer cells compared to NHOK. In addition, the level of SM was decreased in most of the HNSCC cells.

3.3 HNSCC cells have altered glucose metabolism

One of the hallmarks of cancer is an altered glucose metabolism. Most cancer cells have a high rate of aerobic glycolysis (Warburg effect) for the generation of ATP, resulting in increased lactate production; mechanisms essential for their continued uncontrolled growth and cell proliferation (Hsu and Sabatini, 2008). In addition to the production of metabolic energy, glucose degradation provides cancer cells with intermediates needed for biosynthetic pathways and therefore the Warburg effect benefits cancer cells both with bioenergetics and biosynthesis (Heiden et al., 2009). Our results showed significantly elevated levels of lactate

in most of the HNSCC cells (UM-SCC-1, HSC-3, UM-SCC-17B) compared to NHOK, which can be attributed to consequences of the Warburg effect. On the other hand, two HNSCC cells (UM-SCC-14A, OSCC-3) showed significantly decreased levels of lactate as compared to NHOK. The decrease in lactate levels could be hypothesized as a metabolic switch from the Warburg effect to oxidative phosphorylation (Pasteur's effect) in order to furnish ATP, wherein cancer cells utilize lactate for oxidative phosphorylation via monocarboxylate transporters (MCTs) (Semenza, 2008). MCTs, a family of membrane proteins, are critical for metabolic communication between cells, and are involved in intracellular pH regulation by the co-transport of monocarboxylates, such as lactate, pyruvate and ketone bodies. Lactate production, due to the high glycolytic rates in cancer cells, enhances intracellular acidosis, which in turn leads to apoptosis. To prevent apoptosis by intracellular acidosis and allow maintenance of glycolytic rates, it is expected that MCTs would be up-regulated in cancer cells. Significantly higher as well as lower lactate levels observed in HNSCC cells reveal that an altered glucose metabolism in these glycolytic phenotypes could be facilitated by either the Warburg effect or Pasteur's effect. In addition, significant accumulation of phosphagen metabolites, such as creatine and phosphocreatine, in one or more HNSCC cells suggests an enhanced energy metabolism, and thus programming for rapid cell proliferation (Cairns et al., 2011).

Elevated levels of UDP-sugars (UDP-GlcNAc and UDP-GalNAc), the metabolites involved in the hexosamine biosynthetic pathway, are observed in most of the HNSCC cells. Increased levels of UDP-sugars could be due to an up-regulation of a glucose flux, which varies in different cell types. Moreover, these metabolites are involved in the biosynthesis of complex extracellular N-glycans and O-GlcNAcylation (Slawson et al., 2010). It has been suggested that increases in O-GlcNAcylation could be beneficial to the progression of cancer cells (Slawson et al., 2010, Lau and Dennis, 2008); however, the role of the hexosamine biosynthetic pathway in head and neck cancer needs further investigation. By and large, HNSCC cells exhibit an enhanced glycolytic flux to produce ATP for energy requirements, and rapid cell proliferation and growth. Therefore, exploring glycolytic enzyme inhibitors (Pathania et al., 2009) could be advantageous in head and neck cancer therapy.

3.4 TCA cycle anaplerotic flux: amino acid metabolism

Increased levels of leucine, isoleucine, valine, phenylalaine and tyrosine were observed in one or more HNSCC cells. These metabolites were involved in anaplerosis, in which phenylalanine and tyrosine, and isoleucine and valine enter the TCA cycle by converting into fumarate and succinyl Co-A, respectively (Owen et al., 2002). Moreover, the ratio of glutamate:glutamine was elevated in most of the HNSCC cells as compared to NHOK (Fig. 4C), suggesting an increased conversion of glutamine to glutamate (glutaminolysis) in HNSCC cells via glutaminase. Glutamate is further converted to α-ketoglutarate, a key oxidative substrate for the TCA cycle (Dang, 2010b). The role of glutaminolysis to provide anaplerotic carbons through the TCA cycle has been well documented in many cancer types (Dang, 2010a, Simpson et al., 2011, Denkert et al., 2008), nevertheless its biological importance in HNSCC needs further investigations. Elevated levels of these metabolites suggest a high anaplerotic flux, a critical feature of tumor cell growth metabolism, which enables cells to use the TCA cycle as a supply of biosynthetic precursors. In addition, a significant decrease in the levels of aspartate in all the HNSCC cells was observed, which may result from the activity of the aspartate/malate shuttle, further underscoring dysregulation of TCA activity in these cancer types. Furthermore, elevated levels of these amino acids were in accordance with our previous NMR study on human HNSCC tissues relative to matched normal tissues (Somashekar et al., 2011).

3.5 Membrane choline-phospholipid metabolism (MCPM)

It has been well established that choline phospholipid metabolism is altered in most cancer types, wherein cancer cells exhibit altered levels of choline-containing compounds, such as PC, LysoPC, GPC and PCho (Aboagye and Bhujwalla, 1999). An altered MCPM has been a common feature of cancer with consequent alterations of these choline-containing metabolites (Glunde and Serkova, 2006) in which the production of these metabolites is facilitated by the activation of both biosynthetic (*choline kinase*) as well as catabolic (*Phospholipases A, C and D*) enzymes. In the present study, to examine the complete MCPM, we traced the dynamic regulation of choline-containing compounds in HNSCC cells both by ^{1}H NMR of the lipid extract as well as the aqueous extract. The ^{1}H NMR of the lipid extract revealed that the PC:LysoPC ratio was significantly decreased ($P < 0.001$) in all the HNSCC cells compared to NHOK (Fig 5A and B), which clearly demonstrates an increase in the conversion of PC to LysoPC. Consequently, the level of arachidonic acid was significantly increased in all the HNSCC cells (Fig 5A and B). The biochemical hydrolysis of glycerophospholipids at the *sn-2* bond to release lysophospholipid and fatty acid is facilitated by the enzyme *phospholipase* A_2 (PLA_2). It has been well documented in cancer biology that the expression and the activity of PLA_2 is significantly increased in several cancer types (Cummings, 2007), however it has not been well explored previously in HNSCC biology. PLA_2 isozymes occur in fifteen groups comprising three main types, including $sPLA_2$, $cPLA_2$ and $iPLA_2$ (Adibhatla et al., 2003, Burke and Dennis, 2009). In particular, several studies have demonstrated that $cPLA_2$ specifically cleaves the acyl ester bond of PC to generate LysoPC and release arachidonic acid (Linkous and Yazlovitskaya, 2010, Lim et al., 2010, Adibhatla et al., 2006). The elevated levels of LysoPC and arachidonic acid observed in HNSCC cells further support the need to explore the activity of PLA_2 and $cPLA_2$. It was clearly observed that all the HNSCC cell types showed significantly increased activity of PLA_2 as well as $cPLA_2$ compared to NHOK (Fig. 6A and B). The metabolomic findings from the NMR data, coupled with the PLA_2 and $cPLA_2$ activity assays demonstrate that the simultaneous decrease in the PC:LysoPC ratio as well as an increase in arachidonic acid observed in HNSCC cells can be attributed to the increased activity of $cPLA_2$. Further, arachidonic acid, in the presence of *lipoxygenases* and *cyclooxygenases* metabolizes into several molecules such as leukotrienes, prostaglandins and thromboxanes, which induce cancer cell growth and inflammation (Cummings, 2007, Linkous and Yazlovitskaya, 2010, Harris, 2007).

From the ^{1}H NMR spectra of aqueous extracts, increased PCho:GPC ratios were observed in most of the HNSCC cells compared to NHOK (Fig 4D and 4E), however total choline-containing compounds (tCho) were elevated in all the HNSCC cells (Fig 4D), which is a typical characteristic of most cancer types, including breast, prostate and ovarian cancer (Glunde et al., 2006). A dynamic metabolic switch from high GPC to low PCho (PCho:GPC < 1) and conversely high PCho to low GPC (PCho:GPC > 1) could be related to malignant phenotypes associated with altered MCPM. The cancer phenotypes of PCho:GPC > 1 were also observed in oncogenically-transformed and human breast tumor cell lines (Aboagye and Bhujwalla, 1999). We hypothesize that some of the HNSCC cells similarly adopt a “GPC-to-PCho” metabolic switch for the biosynthesis of their cell membranes for rapid growth and proliferation. On the other hand, the HNSCC phenotypes with a PCho:GPC < 1 could be attributed to a reduction in phosphatidylcholine turnover (Podo, 1999), which is opposite to that observed in the other three HNSCC cells and, breast, prostate and ovarian cancer cells. Elevated levels of choline-containing compounds were also observed in our recent *ex vivo* NMR study of HNSCC tissues (Somashekar et al., 2011), which agrees with our present observations. Understanding the molecular regulation of choline-containing metabolites involved in altered choline phospholipid metabolism (Fig. 6B) may help to elucidate aspects of HNSCC biology, and could be helpful in the development of targeted anticancer

therapies. The increased activity of total PLA_2 and specifically the isoform $cPLA_2$ (Fig. 6B), which induce cancer cell growth may be targets for anti-head and neck cancer drugs (Cummings, 2007).

3.6 Osmo-regulatory adaptive mechanisms

All the HNSCC cells showed significantly increased taurine levels compared to NHOK, which is in accordance with the elevated taurine levels observed in our previous NMR study of HNSCC tissues (Somashekar et al., 2011). The β-amino acid taurine is an osmoprotectant, and as such is known to be a substrate for the volume-activated organic osmolyte efflux pathway (Kirk, 1997, Lambert, 2004). With a change in the hydration state of cells (cellular swelling), cells are able to regulate their volume by mediating a net efflux or uptake of osmolytes (Hoffmann and Simonsen, 1989). However, the selection of osmolytes depends on the duration of the osmotic stress, the availability of substrates and osmolytes in the tumor microenvironment. In addition to osmoregulation, taurine is also found to display antineoplastic and antioxidant properties (El Agouza et al., 2011). Due to the multiple functions of taurine in tumor cells, its exact role in head and neck cancer is unclear. Nevertheless, taurine has been suggested as a biomarker of various cancers including hepatocellular carcinoma (El Agouza et al., 2011), breast cancer (El Agouza et al., 2011) and bladder cancer (Srivastava et al., 2010).

Myo-inositol, another osmolyte known to be associated with osmo- and volume regulation (Griffin and Shockcor, 2004), is also significantly increased in most of the HNSCC cell lines. Elevated levels of *myo*-inositol have been observed in various cancers types, including glioma (Castillo et al., 2000) and ovarian (Ferretti et al., 2002). However, decreased levels of *myo*-inositol have also been reported in breast (Beckonert et al., 2003) and prostate cancer (Serkova et al., 2008). In addition to its osmoprotectant property, *myo*-inositol has also been associated with phosphatidycholine turnover and modulation of phospholipids (phosphatidylinositol) in mammalian cells (Lodi et al., 2011). Based on the fact that both taurine and *myo*-inositol are elevated in most of the HNSCC cells, it can be hypothesized that these cells experience cell volume perturbation leading to protective and adaptive mechanisms potentially facilitated by the increased expression of the *myo*-inositol cotransporter (SMIT) and taurine transporter (TauT) (Hoffmann et al., 2009). Increased expression of the *myo*-inositol transporter SLC2A13 observed in primary cultures of oral squamous cell carcinoma cells (Lee et al., 2011) further supports our observation of elevated *myo*-inositol levels.

3.7 Antioxidant defense mechanisms

Significantly increased GSH levels were observed in most of the HNSCC cells. GSH, a ubiquitous intra- and extracellular protective antioxidant, plays a key role against pro-inflammatory processes. Several studies revealed that cancer cells undergo increased oxidative stress associated with malignant transformation, alterations in metabolic activity, and increased generation of reactive oxygen species (Pelicano et al., 2004). The onset of oxidative stress in cancer cells causes elevated expression of antioxidant enzymes, such as glutathione peroxidase, glutathione reductase and glutathione-S-transferase (Meister and Anderson, 1983). The elevated expression of GSH was also observed in our recent NMR studies on HNSCC tissues (Somashekar et al., 2011). In addition, high GSH, glutathione peroxidase and glutathione reductase were reported in the tissues of oral squamous cell carcinoma (Wong et al., 1994, Fiaschi et al., 2005), and other various human cancers, such as colorectal, breast, ovarian and brain tumors (Pelicano et al., 2004). Therefore, the elevated GSH levels could be related to enhanced antioxidant mechanisms in HNSCC cells.

4. Conclusions

In summary, we probed the global metabolic profiling of both polar and non-polar metabolites in HNSCC cells derived from various sites of the upper aerodigestive tract and normal human oral keratinocytes using NMR spectroscopy. The ^{1}H NMR spectra of cell extracts clearly differentiated the metabolic phenotypes of normal and HNSCC cells, which provided useful information for defining possible molecular pathways involved in malignant transformation of head and neck cancer. HNSCC cellular profiles are highlighted by altered levels of a wide range of metabolites such as lactate, aspartate, isoleucine, taurine, tyrosine, acetate, NAD^{+}, valine, creatine, *myo*-inositol, alanine, glutamine, UDP-sugars, glutathione, AMP/ADP, phenylalanine, glycine and fumarate. These metabolites, which are associated with malignant transformation of head and neck neoplasia, can be related to dysregulation of aerobic glycolysis (Warburg effect), oxidative phosphorylation (Pasteur's effect), energy metabolism, the hexosamine pathway, TCA cycle anaplerosis, and osmo-regulatory and anti-oxidant mechanisms. To examine the entire MCPM pathway, we analyzed PC, LysoPC (from NMR of lipid extracts), GPC, PCho and Cho (from NMR of aqueous extracts). Significant alterations in the PC:LysoPC and PCho:GPC ratios observed in all the HNSCC cells suggest an over-expression of phospholipases, which are known to promote cancer cell growth. The increased activity of PLA_2, particularly $cPLA_2$ in all the HNSCC cells observed in the present study further supports increased hydrolysis of PC to LysoPC. Since the MCPM pathway is highly active in HNSCC, the efficacy of anti-cancer drugs targeting phospholipases can be further explored. The global metabolic profiling presented here is useful in monitoring molecular mechanisms in response to chemotherapy, and in this respect, our ongoing studies are focused on monitoring the anti-cancer efficacy of diverse antimicrobial peptides (Hoskin and Ramamoorthy, 2008).

Supplementary Material

Refer to Web version on PubMed Central for supplementary material.

Acknowledgments

This research was supported by funds from NIH (RR023587 and partly GM095640 to A. R and R01DE014429 and R56DE014429 to Y.L.K).

References

Aboagye EO, Bhujwalla ZM. Malignant transformation alters membrane choline phospholipid metabolism of human mammary epithelial cells. Cancer Research. 1999; 59:80–84. [PubMed: 9892190]

Adibhatla RM, Hatcher JF, Dempsey RJ. Phospholipase A(2), hydroxyl radicals, and lipid peroxidation in transient cerebral ischemia. Antioxidants & Redox Signaling. 2003; 5:647–654. [PubMed: 14580322]

Adibhatla RM, Hatcher JF, Larsen EC, Chen XZ, Sun DD, Tsao FHC. CDP-choline significantly restores phosphatidylcholine levels by differentially affecting phospholipase A(2) and CTP: Phosphocholine cytidylyltransferase after stroke. Journal of Biological Chemistry. 2006; 281:6718–6725. [PubMed: 16380371]

Adosraku RK, Choi GTY, Constantinoukokotos V, Anderson MM, Gibbons WA. Nmr Lipid Profiles of Cells, Tissues, and Body-Fluids - Proton Nmr Analysis of Human Erythrocyte Lipids. Journal of Lipid Research. 1994; 35:1925–1931. [PubMed: 7868971]

Alhazzazi TY, Kamarajan P, Joo N, Huang JY, Verdin E, D'Silva NJ, Kapila YL. Sirtuin-3 (SIRT3), a novel potential therapeutic target for oral cancer. Cancer. 2011; 117:1670–1678. [PubMed: 21472714]

Argiris A, Karamouzis MV, Raben D, Ferris RL. Head and neck cancer. Lancet. 2008; 371:1695–1709. [PubMed: 18486742]

Beckonert O, Monnerjahn K, Bonk U, Leibfritz D. Visualizing metabolic changes in breast-cancer tissue using H-1-NMR spectroscopy and self-organizing maps. Nmr in Biomedicine. 2003; 16:1–11. [PubMed: 12577292]

Benjamini Y, Hochberg Y. Controlling the False Discovery Rate - a Practical and Powerful Approach to Multiple Testing. Journal of the Royal Statistical Society Series B-Methodological. 1995; 57:289–300.

Blaise BJ, Shintu L, Elena B, Emsley L, Dumas ME, Toulhoat P. Statistical recoupling prior to significance testing in nuclear magnetic resonance based metabonomics. Anal Chem. 2009; 81:6242–6251. [PubMed: 19585975]

Burke JE, Dennis EA. Phospholipase A(2) structure/function, mechanism, and signaling. Journal of Lipid Research. 2009; 50:S237–S242. [PubMed: 19011112]

Cairns RA, Harris IS, Mak TW. Regulation of cancer cell metabolism. Nature Reviews Cancer. 2011; 11:85–95.

Castillo M, Smith JK, Kwock L. Correlation of myo-inositol levels and grading of cerebral astrocytomas. American Journal of Neuroradiology. 2000; 21:1645–1649. [PubMed: 11039343]

Cui Q, Lewis IA, Hegeman AD, Anderson ME, Li J, Schulte CF, Westler WM, Eghbalnia HR, Sussman MR, Markley JL. Metabolite identification via the Madison Metabolomics Consortium Database. Nat Biotechnol. 2008; 26:162–164. [PubMed: 18259166]

Cummings BS. Phospholipase A(2) as targets for anti-cancer drugs. Biochemical Pharmacology. 2007; 74:949–959. [PubMed: 17531957]

Dang CV. Glutaminolysis: supplying carbon or nitrogen or both for cancer cells? Cell Cycle. 2010a; 9:3884–3886. [PubMed: 20948290]

Dang CV. Rethinking the Warburg effect with Myc micromanaging glutamine metabolism. Cancer Res. 2010b; 70:859–862. [PubMed: 20086171]

Denkert C, Budczies J, Weichert W, Wohlgemuth G, Scholz M, Kind T, Niesporek S, Noske A, Buckendahl A, Dietel M, Fiehn O. Metabolite profiling of human colon carcinoma--deregulation of TCA cycle and amino acid turnover. Mol Cancer. 2008; 7:72. [PubMed: 18799019]

El Agouza IM, Eissa SS, El Houseini MM, El-Nashar DE, Abd El Hameed OM. Taurine: a novel tumor marker for enhanced detection of breast cancer among female patients. Angiogenesis. 2011; 14:321–330. [PubMed: 21553281]

Ferretti A, D'Ascenzo S, Knijn A, Iorio E, Dolo V, Pavan A, Podo F. Detection of polyol accumulation in a new ovarian carcinoma cell line, CABA I: a H-1 NMR study. British Journal of Cancer. 2002; 86:1180–1187. [PubMed: 11953869]

Fiaschi AI, Cozzolino A, Ruggiero G, Giorgi G. Glutathione, ascorbic acid and antioxidant enzymes in the tumor tissue and blood of patients with oral squamous cell carcinoma. European review for medical and pharmacological sciences. 2005; 9:361–367. [PubMed: 16479741]

Glunde K, Ackerstaff E, Mori N, Jacobs MA, Bhujwalla ZM. Choline phospholipid metabolism in cancer: consequences for molecular pharmaceutical interventions. Mol Pharm. 2006; 3:496–506. [PubMed: 17009848]

Glunde K, Serkova NJ. Therapeutic targets and biomarkers identified in cancer choline phospholipid metabolism. Pharmacogenomics. 2006; 7:1109–1123. [PubMed: 17054420]

Griffin JL, Shockcor JP. Metabolic profiles of cancer cells. Nature Reviews Cancer. 2004; 4:551–561.

Harris RE. Cyclooxygenase-2 (cox-2) and the inflammogenesis of cancer. Subcell Biochem. 2007; 42:93–126. [PubMed: 17612047]

Heiden MGV, Cantley LC, Thompson CB. Understanding the Warburg Effect: The Metabolic Requirements of Cell Proliferation. Science. 2009; 324:1029–1033. [PubMed: 19460998]

Hoffmann EK, Lambert IH, Pedersen SF. Physiology of Cell Volume Regulation in Vertebrates. Physiological Reviews. 2009; 89:193–277. [PubMed: 19126758]

Hoffmann EK, Simonsen LO. Membrane Mechanisms in Volume and Ph Regulation in Vertebrate Cells. Physiological Reviews. 1989; 69:315–382. [PubMed: 2538851]

Hoskin DW, Ramamoorthy A. Studies on anticancer activities of antimicrobial peptides. Biochim Biophys Acta. 2008; 1778:357–375. [PubMed: 18078805]

Hsu PP, Sabatini DM. Cancer cell metabolism: Warburg and beyond. Cell. 2008; 134:703–707. [PubMed: 18775299]

Jiffar T, Yilmaz T, Lee J, Hanna E, El-Naggar A, Yu D, Myers JN, Kupferman ME. KiSS1 mediates platinum sensitivity and metastasis suppression in head and neck squamous cell carcinoma. Oncogene. 2011; 30:3163–3173. [PubMed: 21383688]

Karahatay S, Thomas K, Koybasi S, Senkal CE, Elojeimy S, Liu X, Bielawski J, Day TA, Gillespie MB, Sinha D, Norris JS, Hannun YA, Ogretmen B. Clinical relevance of ceramide metabolism in the pathogenesis of human head and neck squamous cell carcinoma (HNSCC): attenuation of C(18)-ceramide in HNSCC tumors correlates with lymphovascular invasion and nodal metastasis. Cancer Lett. 2007; 256:101–111. [PubMed: 17619081]

Kirk K. Swelling-activated organic osmolyte channels. Journal of Membrane Biology. 1997; 158:1–16. [PubMed: 9211717]

Lambert IH. Regulation of the cellular content of the organic osmolyte taurine in mammalian cells. Neurochemical Research. 2004; 29:27–63. [PubMed: 14992263]

Lau KS, Dennis JW. N-Glycans in cancer progression. Glycobiology. 2008; 18:750–760. [PubMed: 18701722]

Lee JH, Lee DG, Kim MJ, Kim SM, Li B, Kwon BS. H(+)-myo-inositol transporter SLC2A13 as a potential marker for cancer stem cells in an oral squamous cell carcinoma. Oral Oncology. 2011; 47:S111–S111.

Leemans CR, Braakhuis BJ, Brakenhoff RH. The molecular biology of head and neck cancer. Nat Rev Cancer. 2011; 11:9–22. [PubMed: 21160525]

Lim SC, Cho N, Lee TB, Choi CH, Min YD, Kim SS, Kim KJ. Impacts of Cytosolic Phospholipase A2-15-Prostaglandin Dehydrogenase, and Cyclooxygenase-2 Expressions on Tumor Progression in Colorectal Cancer. Yonsei Medical Journal. 2010; 51:692–699. [PubMed: 20635443]

Linkous A, Yazlovitskaya E. Cytosolic phospholipase A2 as a mediator of disease pathogenesis. Cellular Microbiology. 2010; 12:1369–1377. [PubMed: 20642808]

Lodi A, Tiziani S, Khanim FL, Drayson MT, Gunther UL, Bunce CM, Viant MR. Hypoxia Triggers Major Metabolic Changes in AML Cells without Altering Indomethacin-Induced TCA Cycle Deregulation. Acs Chemical Biology. 2011; 6:169–175. [PubMed: 20886892]

MacKinnon N, Khan AP, Chinnaiyan AM, Rajendiran TM, Ramamoorthy A. Androgen receptor activation results in metabolite signatures of an aggressive prostate cancer phenotype: an NMR-based metabonomics study. Metabolomics. 2012 *Published online: 02 Febrauary*.

Marur S, D'Souza G, Westra WH, Forastiere AA. HPV-associated head and neck cancer: a virus-related cancer epidemic. Lancet Oncol. 2010; 11:781–789. [PubMed: 20451455]

Meister A, Anderson ME. Glutathione. Annu Rev Biochem. 1983; 52:711–760. [PubMed: 6137189]

Owen OE, Kalhan SC, Hanson RW. The key role of anaplerosis and cataplerosis for citric acid cycle function. Journal of Biological Chemistry. 2002; 277:30409–30412. [PubMed: 12087111]

Pathania D, Millard M, Neamati N. Opportunities in discovery and delivery of anticancer drugs targeting mitochondria and cancer cell metabolism. Adv Drug Deliv Rev. 2009; 61:1250–1275. [PubMed: 19716393]

Pelicano H, Carney D, Huang P. ROS stress in cancer cells and therapeutic implications. Drug resistance updates : reviews and commentaries in antimicrobial and anticancer chemotherapy. 2004; 7:97–110. [PubMed: 15158766]

Pignon JP, le Maitre A, Maillard E, Bourhis J. Meta-analysis of chemotherapy in head and neck cancer (MACH-NC): an update on 93 randomised trials and 17,346 patients. Radiother Oncol. 2009; 92:4–14. [PubMed: 19446902]

Podo F. Tumour phospholipid metabolism. Nmr in Biomedicine. 1999; 12:413–439. [PubMed: 10654290]

Rezende TM, de Souza Freire M, Franco OL. Head and neck cancer: proteomic advances and biomarker achievements. Cancer. 2010; 116:4914–4925. [PubMed: 20665484]

Sandulache VC, Ow TJ, Pickering CR, Frederick MJ, Zhou G, Fokt I, Davis-Malesevich M, Priebe W, Myers JN. Glucose, not glutamine, is the dominant energy source required for proliferation and

survival of head and neck squamous carcinoma cells. Cancer. 2011; 117:2926–2938. [PubMed: 21692052]

Schmitz S, Machiels JP. Molecular biology of squamous cell carcinoma of the head and neck: relevance and therapeutic implications. Expert Rev Anticancer Ther. 2010; 10:1471–1484. [PubMed: 20836682]

Semenza GL. Tumor metabolism: cancer cells give and take lactate. Journal of Clinical Investigation. 2008; 118:3835–3837. [PubMed: 19033652]

Serkova NJ, Gamito EJ, Jones RH, O'Donnell C, Brown JL, Green S, Sullivan H, Hedlund T, Crawford ED. The metabolites citrate, myo-inositol, and spermine are potential age-independent markers of prostate cancer in human expressed prostatic secretions. Prostate. 2008; 68:620–628. [PubMed: 18213632]

Simpson NE, Tryndyak VP, Beland FA, Pogribny IP. An in vitro investigation of metabolically sensitive biomarkers in breast cancer progression. Breast Cancer Res Treat. 2011

Slawson C, Copeland RJ, Hart GW. O-GIcNAc signaling: a metabolic link between diabetes and cancer? Trends in Biochemical Sciences. 2010; 35:547–555. [PubMed: 20466550]

Somashekar BS, Kamarajan P, Danciu T, Kapila YL, Chinnaiyan AM, Rajendiran TM, Ramamoorthy A. Magic Angle Spinning NMR-Based Metabolic Profiling of Head and Neck Squamous Cell Carcinoma Tissues. Journal of Proteome Research. 2011

Srivastava S, Roy R, Singh S, Kumar P, Dalela D, Sankhwar SN, Goel A, Sonkar AA. Taurine - a possible fingerprint biomarker in non-muscle invasive bladder cancer: A pilot study by (1)H NMR spectroscopy. Cancer Biomarkers. 2010; 6:11–20. [PubMed: 20164538]

Wishart DS, Tzur D, Knox C, Eisner R, Guo AC, Young N, Cheng D, Jewell K, Arndt D, Sawhney S, Fung C, Nikolai L, Lewis M, Coutouly MA, Forsythe I, Tang P, Shrivastava S, Jeroncic K, Stothard P, Amegbey G, Block D, Hau DD, Wagner J, Miniaci J, Clements M, Gebremedhin M, Guo N, Zhang Y, Duggan GE, Macinnis GD, Weljie AM, Dowlatabadi R, Bamforth F, Clive D, Greiner R, Li L, Marrie T, Sykes BD, Vogel HJ, Querengesser L. HMDB: the Human Metabolome Database. Nucleic Acids Res. 2007; 35:D521–D526. [PubMed: 17202168]

Wong DY, Hsiao YL, Poon CK, Kwan PC, Chao SY, Chou ST, Yang CS. Glutathione concentration in oral cancer tissues. Cancer letters. 1994; 81:111–116. [PubMed: 8012928]

Ziebart T, Walenta S, Kunkel M, Reichert TE, Wagner W, Mueller-Klieser W. Metabolic and proteomic differentials in head and neck squamous cell carcinomas and normal gingival tissue. J Cancer Res Clin Oncol. 2011; 137:193–199. [PubMed: 20383719]

Highlights

- Delineation of multiple deregulated metabolic events in head and neck squamous cell carcinoma (HNSCC).
- Glutaminolysis, a major carbon source in HNSCC.
- HNSCC highlighted with altered levels of choline containing metabolites and *phospholipase A_2*, particulary *cytosolic PLA_2 ($cPLA_2$)* revealing altered membrane choline phospholipid metabolism.
- Adaptive mechanism of HNSCC to osmotic and oxidative stress.
- *$cPLA_2$*, a potential therapeutic target.

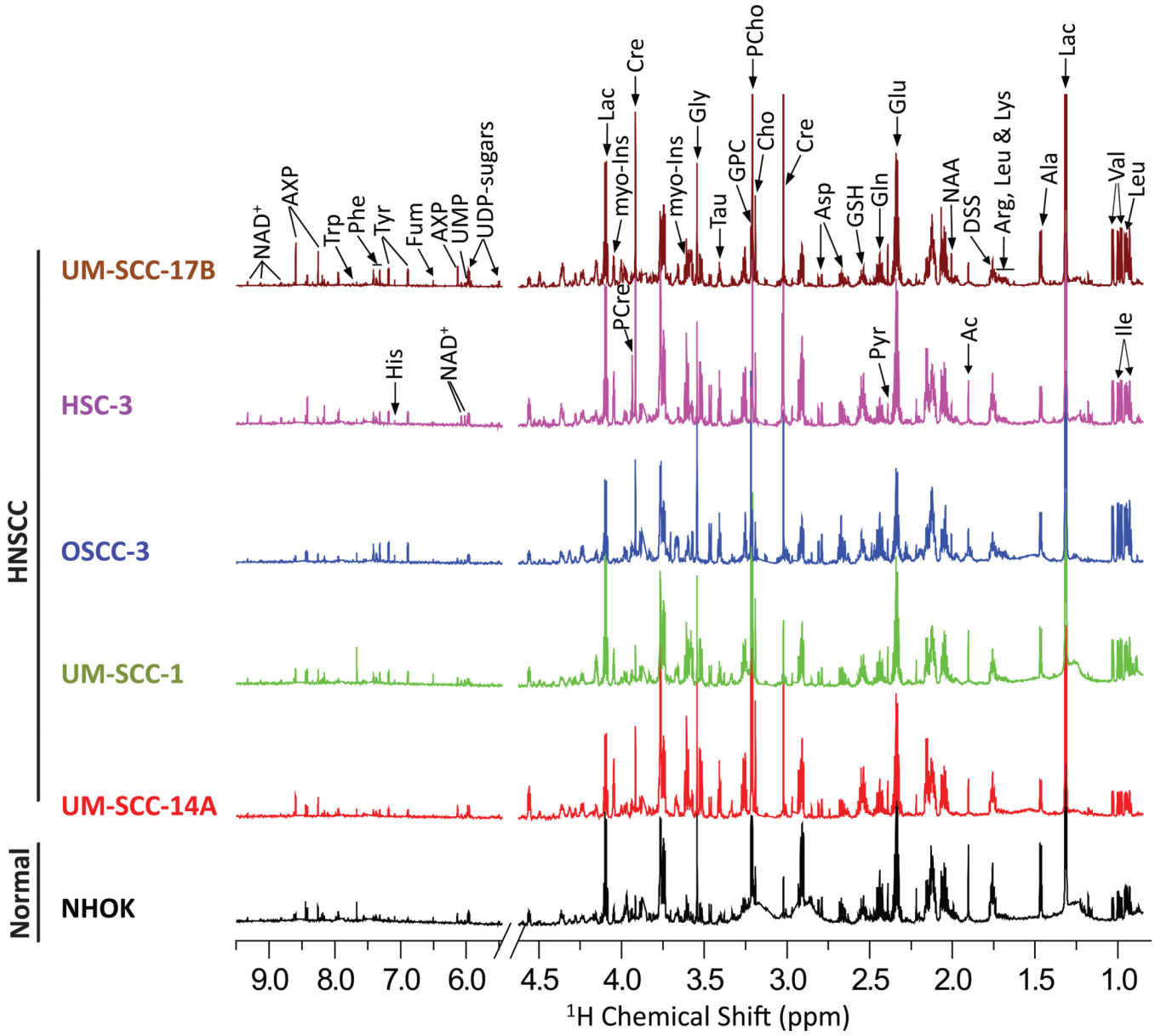

Figure 1.

An average (from triplicates) 900 MHz ^{1}H NMR spectrum (area normalized) acquired on the polar fraction of NHOK cells, and various HNSCC cell types derived from floor of the mouth (UM-SCC-14A and UM-SCC-1), tongue (OSCC-3 and HSC-3) and larynx (UM-SCC-17B). The vertical scales were kept constant in all the ^{1}H NMR spectra. The chemical shift regions of pre-saturated water, HEPES and methanol were removed in all the spectra prior to statistical analysis.

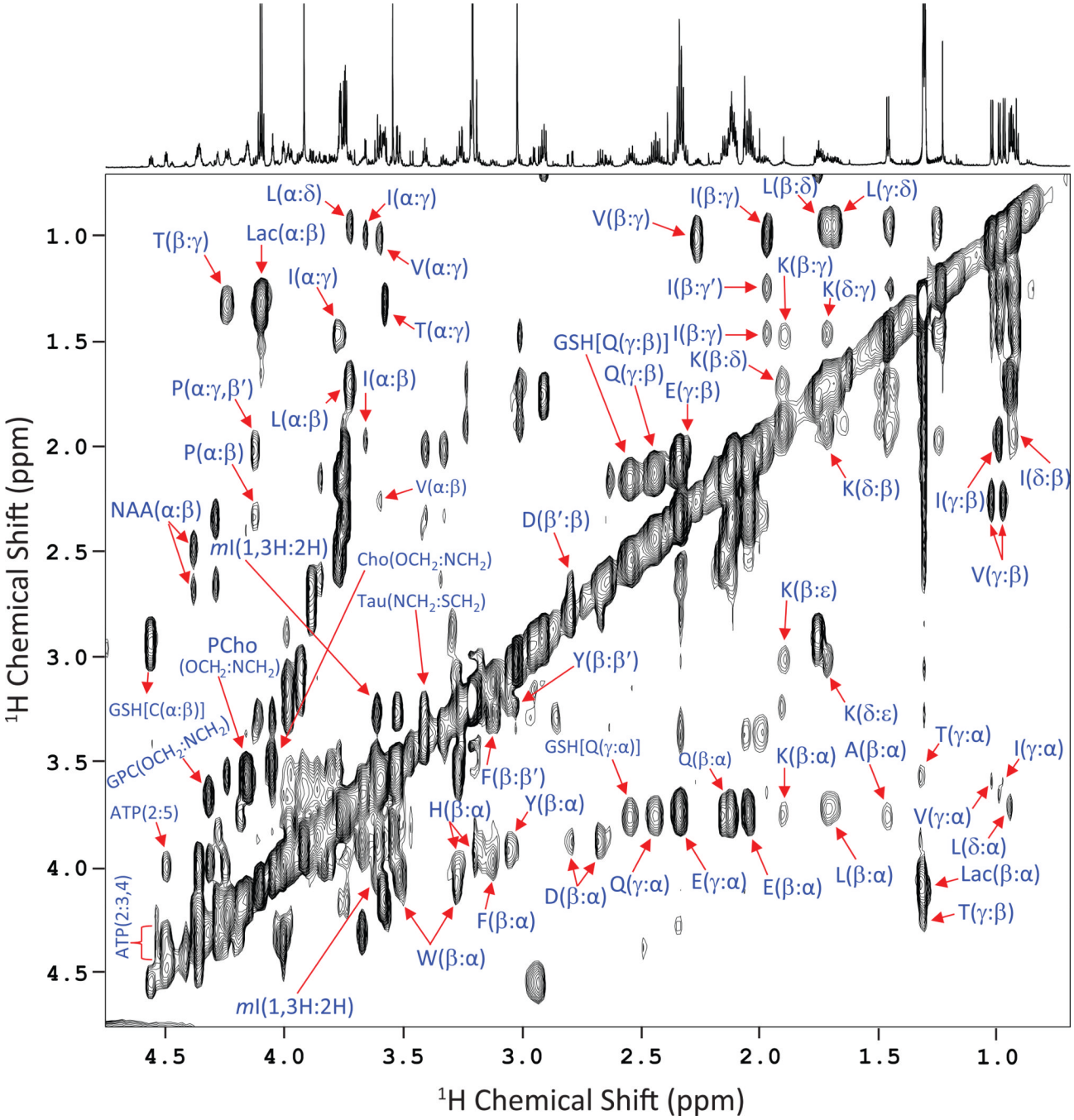

Figure 2.

A representative 900 MHz 2D ^{1}H-^{1}H TOCSY spectrum of one of the HNSCC cell (UM-SCC-17B) samples showing the assignments of various metabolites. The cross peaks between protons of amino acids are marked using single letter codes.

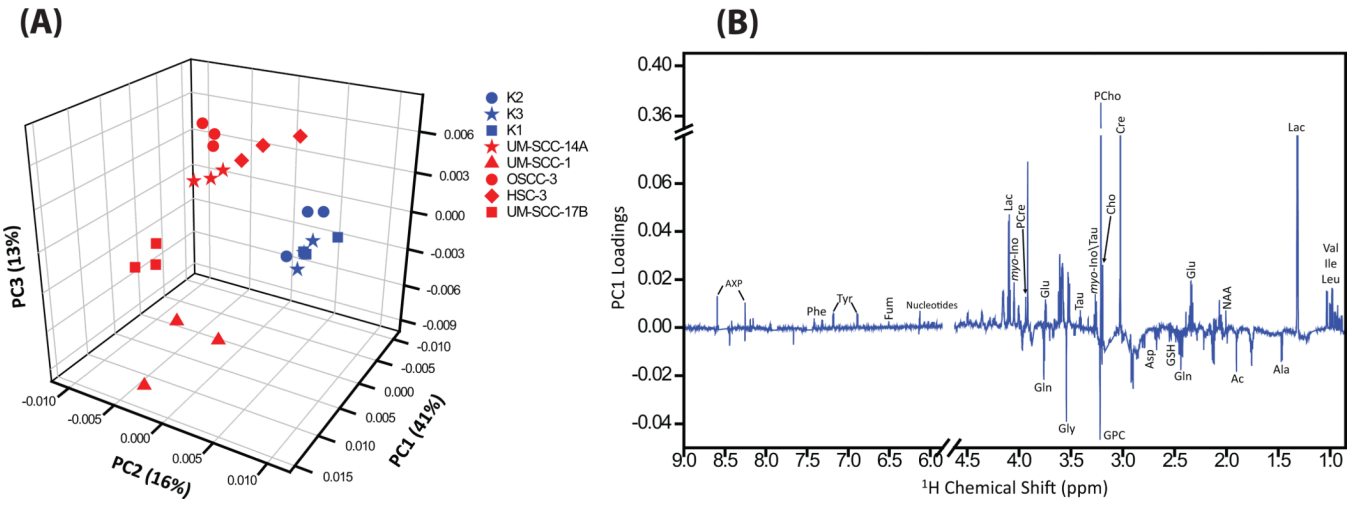

Figure 3.

(A) 3D PCA score plot generated from the unsupervised PCA of NMR spectra of aqueous metabolites showing separate grouping for NHOK and HNSCC cells. The NMR spectra of cells grown independently in triplicates clustered together which reveals the consistent reproducibility of cell growth. The three NHOK showed clear grouping, however the five HNSCC cells showed dispersed cluster due to altered levels of metabolites within cancer group. **(B)** PC1 loadings showing altered metabolites in HNSCC cells.

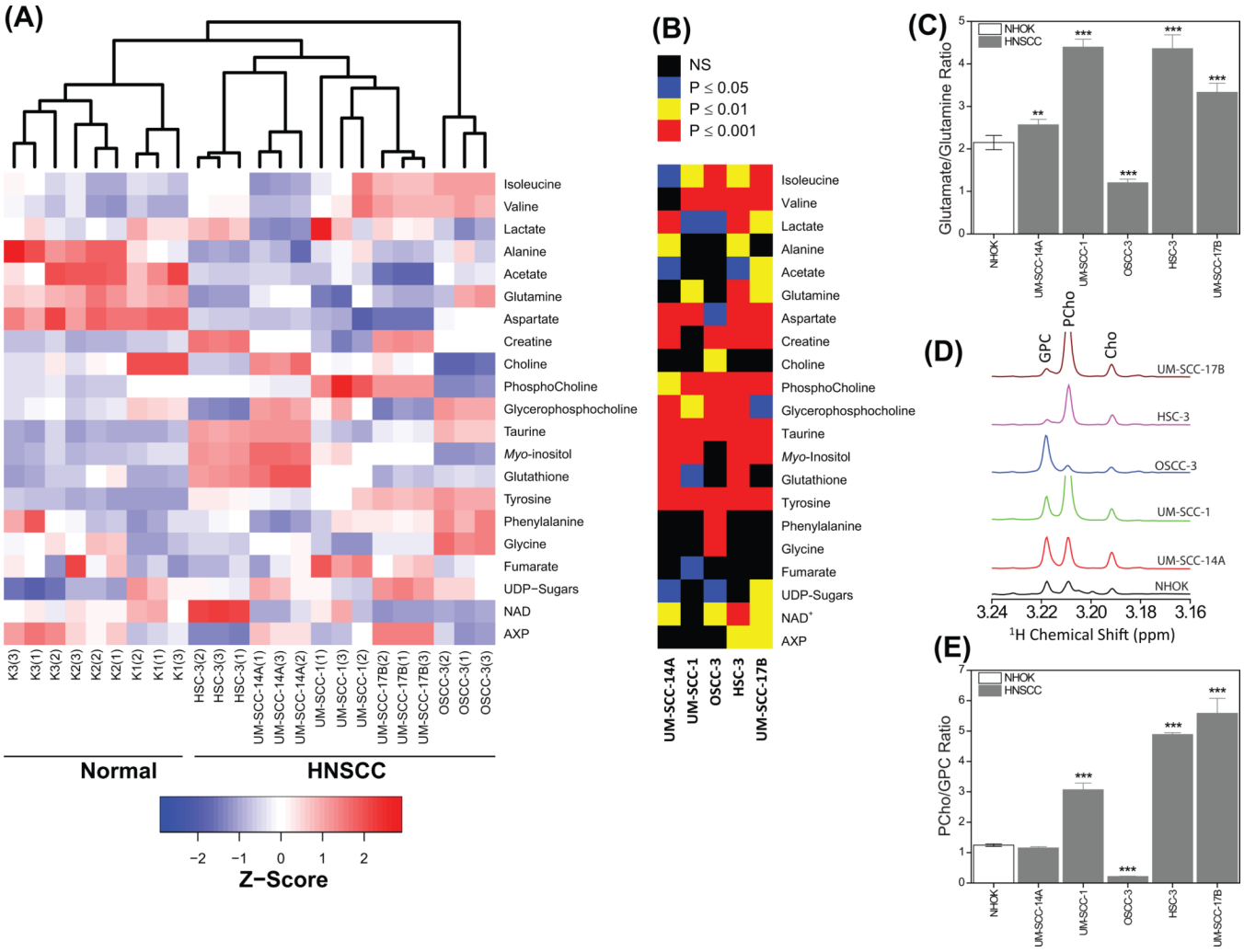

Figure 4.

(A) Heat map showing the z-score of twenty-one quantified metabolites in three NHOK and five HNSCC cells grown independently in triplicates. An unsupervised hierarchical classification showing separate cluster for normal and HNSCC is also included in the heat map. **(B)** *P* values obtained by comparing metabolite levels of normal and HNSCC cells using two-tailed Student's t-test followed by a correction for multiple hypothesis testing (Benjamini-Hochberg correction). **(C)** Bar plots (mean ± SD) showing altered glutamate:glutamine ratio in HNSCC cells compared to NHOK. $^{**}P < 0.01$; $^{***}P < 0.001$. **(D)** Expanded chemical region of $-N(CH_3)_3^+$ signals of choline containing metabolites showing the altered levels of PCho and GPC in HNSCC cells. **(E)** Bar plots (mean ± SD) showing altered PCho:GPC ratio in HNSCC cells compared to NHOK. $^{***}P < 0.001$.

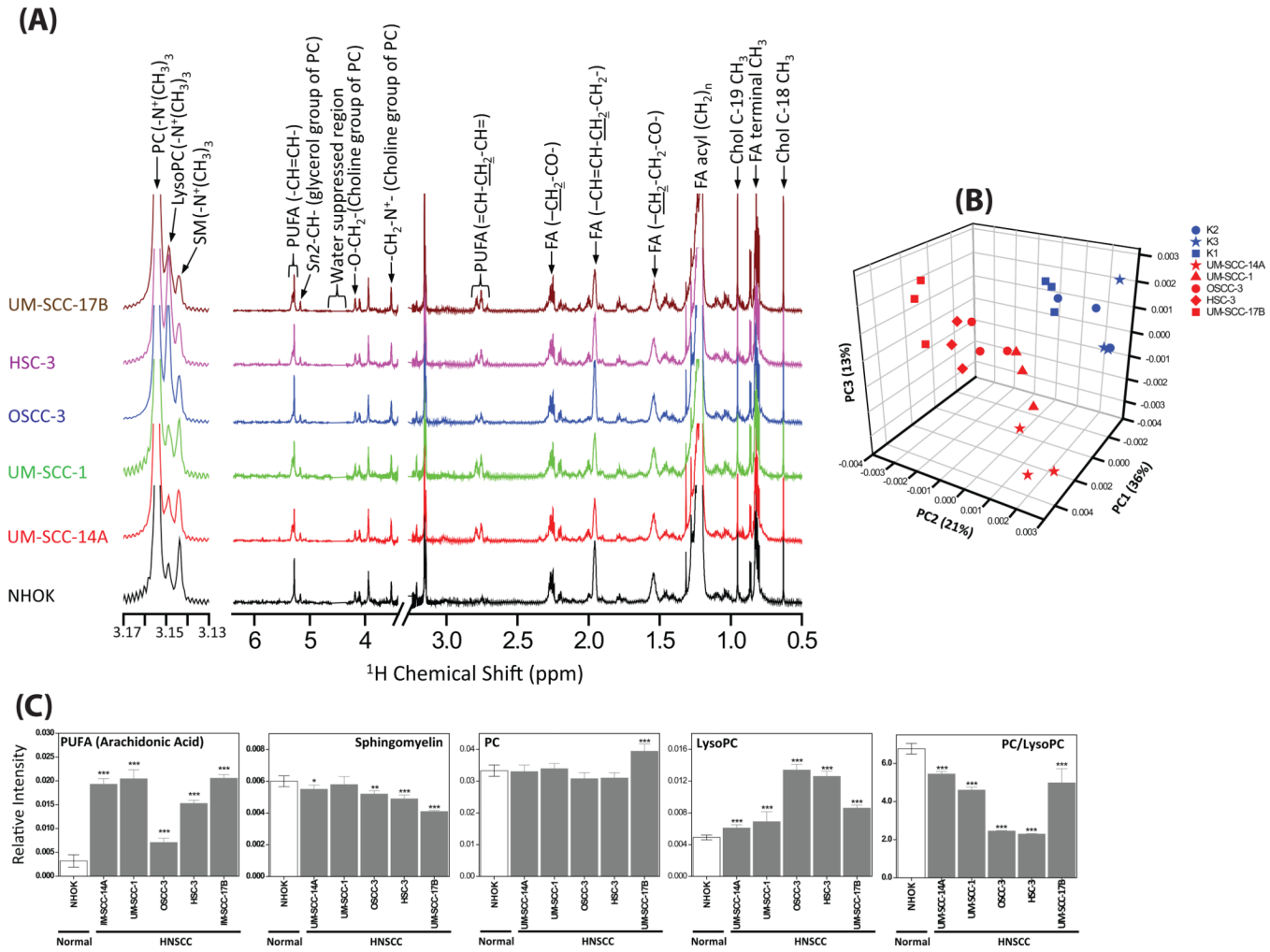

Figure 5.

(A) Average ^{1}H NMR spectra obtained from the area normalized ^{1}H NMR spectrum of lipid extract of each independently grown (triplicates) cells of NHOK and various HNSCC cells. **(B)** 3D PCA score plot generated from the unsupervised PCA of NMR spectra of lipid extracts showing separate grouping for NHOK and HNSCC cells. **(C)** Bar plots showing the comparison (Student's t-test) of relative intensities of cholesterol, poly unsaturated fatty acids (PUFA), sphingomyelin and PC/LysoPC ratio. ***$P < 0.001$; **$P < 0.01$; *$P < 0.05$.

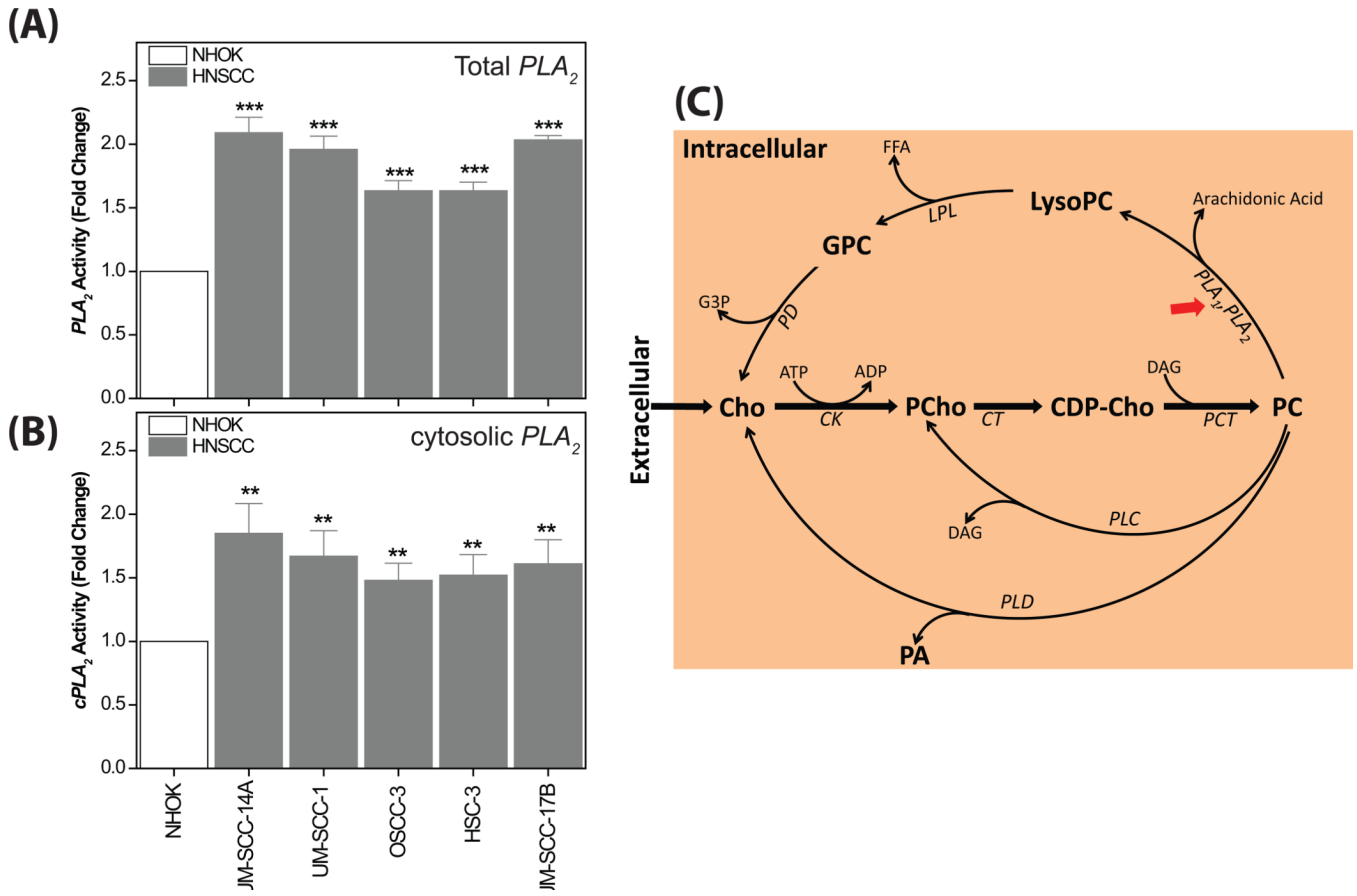

Figure 6.

(A) Bar plots showing significantly increased PLA_2 activity in all the HNSCC cells compared to NHOK. ***$P < 0.001$. **(B)** Bar plots showing significantly increased $cPLA_2$ activity in all the HNSCC cells compared to NHOK. **$P < 0.01$. **(C)** Schematic representation of biosynthesis and hydrolysis of PC in HNSCC effected by three major enzymes, *phospholipase* A_1 and A_2 (PLA_1 and PLA_2), *phospholipase C* (*PLC*) and *phospholipase D* (*PLD*). These *phospholipases* (indicated by red arrows) can be potential drug targets for head and neck cancer. Metabolites: CDP-Cho, cytidine 5`-diphosphocholine; Cho, choline; DAG, diacylglycerol; FFA, free fatty acid; G3P, sn-glycerol-3-phosphate; GPC, glycerophosphocholine; PA, phosphatidic acid; PCho, phosphocholine. Enzymes: *ck, choline kinase; ct, cytidylyltransferase; lpl, lysophospholipase; pct, phosphocholine transferase; pd, glycerophosphocholine phosphodiesterase*.